

# ULTRAFAST TECHNOLOGY APPLIED TO OPTICAL COHERENCE TOMOGRAPHY

BY MATTHEW S. MULLER, PAUL J.L. WEBSTER, VICTOR X.D. YANG AND JAMES M. FRASER

Optical coherence tomography is an imaging modality based on low coherence interferometry, capable of generating *in vivo* three-dimensional images with near cellular resolution at video rates [1]. OCT systems determine path length from light backscattered in a sample by detecting its interference with light returning from a reference arm. Typically, the full three dimensional image is built up by raster scanning in the transverse directions. To retrieve layer depths along an axial line into the sample, two variants of OCT have been developed. Time-domain OCT (TD-OCT) records the total intensity of sample and reference light as a function of reference arm position. By mechanically scanning the reference path delay, the location of interfaces can be determined. Due to its design simplicity and ability to detect retinal tissue damage, TD-OCT had early success in ophthalmic applications but has a limited mechanical scan speed and lower sensitivity relative to other OCT variants [2]. A more recent technique called Fourier-domain OCT (FD-OCT) maintains a stationary reference arm and records the spectral interferogram, either with a spectrometer or a specialised “swept-source” laser that outputs a narrow frequency that varies as a function of time. The full axial image can be retrieved through a Fourier transform of the spectral interferogram, with speeds limited by the electronic capture rate of the imaging spectrum, currently greater than 300kHz for both FD-OCT approaches [3,4].

In most OCT implementations, the transverse and axial resolutions are independent, with the former set by the focussing optics of the probe beam and the latter inversely proportional to the light source bandwidth. Thus the ideal light source for OCT generates a beam of high spatial quality and broad bandwidth with low spectral and random intensity noise. Fibre coupled lamps, superlumi-

nescent diodes, broadband oscillators, nonlinear supercontinuum generators, and swept-source lasers have all been used as broadband light sources for OCT, with typical axial resolutions from 2 to 20  $\mu\text{m}$  [5,6]. Ultrafast light sources are a natural fit, especially in applications that pursue extremely high resolution imaging. Recall that OCT exploits phase delay and not group delay like radar or sonar; the pulsed nature of the ultrafast source is thus irrelevant in standard OCT implementations. The only dispersion requirement for optimal axial resolution is dispersion matching between sample and reference arm. Even if this is not achieved experimentally, electronic dispersion compensation can be implemented in post processing for FD-OCT [7].

We have followed two main research directions involving OCT imaging and ultrafast technology: 1) we exploit the short pulse duration of ultrafast pulses to time gate the light back scattered from a sample of interest to improve imaging contrast, 2) we apply OCT as an *in situ* diagnostic to image ultrafast laser micromachining on microsecond timescales in real time.

## TIME-GATED OPTICAL COHERENCE TOMOGRAPHY

Even with favourable wavelengths for tissue penetration (1050 – 1350 nm [8]), the mean scattering depth of visible and infrared light remains very short. As such, OCT exploits extremely high sensitivities (typically >100 dB) to image several mm into tissue. This is made more challenging by the fact that the coherent signal of interest sits on a large incoherent background. Light scattered from all layers, as well as light that undergoes multiple scattering, is detected, and it is only through numerical post-processing that the small coherent signal is extracted from the background. An important limitation of FD-OCT arises if the sample includes a highly scattering layer (often from the front surface). Saturation of the detector from light from this layer must be avoided or else the interferogram is clipped and the entire axial image is obscured. To avoid saturation, the total signal must be reduced by attenuation of the probe or reference beam intensity, or by a reduction of the detector integration time or gain. Since the detector dynamic range is typically 40-60 dB lower than the overall system sensitivity, the end result is that deeper layers can be masked when a strong scatterer is present. To understand this limitation, an analogy is useful. When you attempt to look through a window at night from a well lit



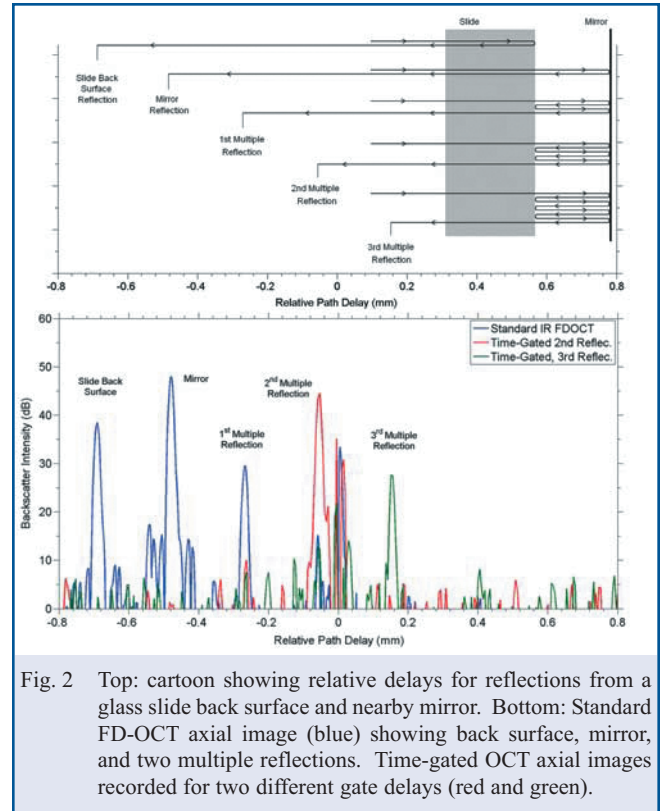
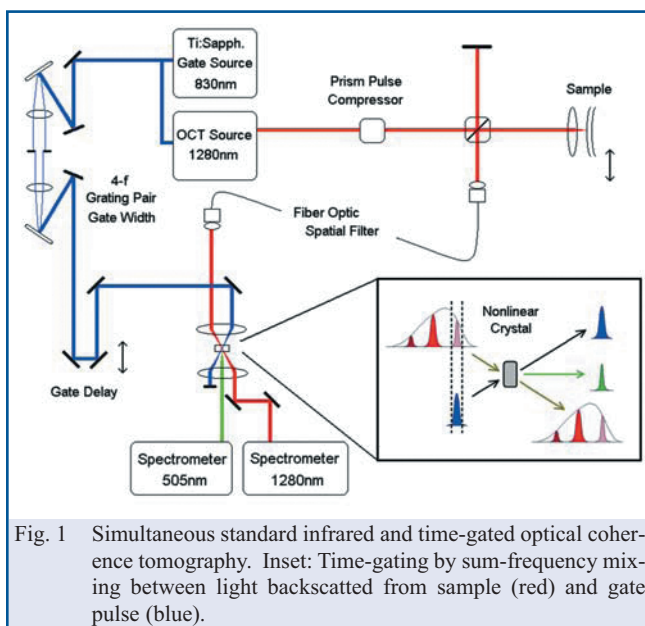
Matthew Muller, recently graduated from Queen's Univ., is now a research associate at the School of Optometry, Indiana University. Paul Webster is a doctoral student and James Fraser <james.fraser@queensu.ca> is an Assistant Professor in the Dept. of Physics, Engineering Physics and Astronomy, Queen's University. Victor Yang is an Assistant Professor in the Department of Electrical and Computer Engineering, Ryerson University.

### SUMMARY

**By time gating with ultrafast optical pulses, we improve optical coherence tomography imaging contrast by 29 dB in a model system. In parallel work, we exploit OCT as an *in situ* diagnostic for ultrafast laser micromachining, to image sample morphology changes on microsecond timescales in real time.**

room, the reflection from the window surface obscures the streetscape outside, even if it is illuminated with streetlamps. By switching off the lights in the room, you turn off the reflection from the window, thus allowing you to make use of your vision's full sensitivity to see outside. In standard OCT, only one source illuminates the entire sample and it is not possible to selectively turn off bright scatterers.

To overcome this problem, we add a temporal filter sensitive to group delay, in combination with the OCT system. This allows us to time gate the backscattered light so that only light from the desired depth of view is detected and processed [9]. By overlapping a user controllable gate pulse with the light returning from the region of interest, the detected signal is restricted to the desired region. We accomplish time gating by sum-frequency mixing between light backscattered from sample (red) and gate pulse (blue) in a nonlinear crystal outside the sample (Fig. 1). The nonlinear mixing process is intensity dependent so that only the backscattered light that overlaps in time with the gate pulse is upconverted into the visible (inset of Fig. 1). Image retrieval is then accomplished using standard FD-OCT post-processing on the upconverted spectrum (centre wavelength 505 nm). The gate delay can be controlled by the user to select a particular region of the sample for viewing. The duration of the time gate, and consequently the width of the viewed region, is controlled by limiting the gate pulse bandwidth in a 4-f grating pair. Since the upconverted depth of field is considerably restricted as compared to standard FD-OCT, the number of sampling points required to avoid aliasing is also reduced, allowing faster acquisition speed and processing. Time-gating has the additional advantage that the upconverted light is in the visible, permitting the use of superior silicon-based CCD technology for detection. The improved detector sensitivity makes up partially for the power loss from the nonlinear mixing process.



Time-gated FD-OCT is demonstrated and compared with standard FD-OCT (provided by the 1280 nm spectrometer also shown in Fig. 1) by recording axial images from a model system. Multiple reflections between a glass slide and a closely spaced mirror provide a useful case study (Fig. 2). Each subsequent reflection is delayed in time and reduced in intensity due to Fresnel reflection losses. The image contrast (maximum to minimum detectable signal) with standard infrared FD-OCT is limited by the dynamic range of the detector array due to the strong reflection from the mirror. Only the first two multiple reflections can be seen above the signal floor (Fig. 2 bottom – blue curve). The signal at zero delay is the DC artefact common to FD-OCT images. By setting the time gate to  $-50 \mu\text{m}$ , the sum-frequency stage restricts the depth field of view to around the second multiple reflection. The strong signal from the mirror is filtered out completely and the feature due to the second reflection is improved by 29 dB compared to standard FD-OCT. The third multiple reflection is completely below the minimum detectable signal viewable with standard FD-OCT system. In time-gated OCT, it can be clearly imaged.

Time-gated FD-OCT can be thought of as a hybrid of OCT and nonlinear microscopy. Two-photon, second-, third- harmonic generation, and CARS microscopy all exploit nonlinear light-matter interaction within the sample to extract information from (primarily) the focal volume of the imaging beam. By contrast, time-gated FD-OCT isolates the layer of interest by nonlinear sum-frequency mixing in a stage external to the sample. This difference allows nonlinear microscopy to achieve

better resolution and chemical sensitivity, but at a cost of requiring high peak irradiance in the sample. Since the spectral interferogram in time-gated FD-OCT does not depend on the phase relation between different frequencies, the pulse can be broadened in time before the sample (using a prism pair, for example) to avoid nonlinear and potentially damaging tissue interactions. Time-gating does require that chirp be compensated before the nonlinear crystal, but in our implementation this is easily achieved with an optical fibre.

We have applied time-gated FD-OCT to image a highly scattering medium (onion), which provided clear observations of cellular structure at penetration depths over 1 mm that match those seen by standard FD-OCT<sup>[10]</sup>. Full realization of the potential of this new technique requires improved nonlinear conversion and/or detection efficiency. Modern nonlinear crystal design (with appropriate poling) would likely achieve better conversion efficiency than the present system time gate. Improved sensitivity with either electron multiplying technology or an avalanche photodiode or photomultiplier tube array has the potential to dramatically improve time-gated sensitivity and speed, potentially surpassing the sensitivity limit of current OCT devices. This technique might find particular relevance as a complementary imaging modality in facilities that already exploit ultrafast technology for imaging.

## OCT IMAGING OF ULTRAFAST LASER MICRO-MACHINING

Ultrafast technology is of considerable interest for laser micromachining precise components such as medical devices or even in cutting tissue (the so-called “photon scalpel”). For example, the mechanical microkeratome blade in LASIK eye surgery is sometimes replaced by an ultrafast laser for producing the initial corneal flap. Generally, due to the nonlinear nature of the process, less heat is deposited into the material and cutting damage is restricted to a smaller volume than compared to traditional “long” pulse laser cutting<sup>[11]</sup>. Being able to follow sample morphology changes throughout the entire cutting process would help further our understanding of this extreme light-matter interaction as well as provide a useful diagnostic to optimize machining parameters and control cutting outcomes. We exploit the high imaging rates of FD-OCT to monitor morphology changes *in situ*. By keeping the imaging beam stationary, we sacrifice full 3D tomography to observe microsecond dynamics along one axial line in real time. Real time imaging is of particular importance for dynamics that have a large degree of variability due to sample inhomogeneities or the stochastic nature of the process itself. With a coaxial alignment of the cutting and imaging beam, the formation of high aspect ratio holes can be easily imaged. In addition, the wavelength selectivity and phase dependence of OCT reduces blinding from the cutting beam and plasma emission.

We have demonstrated the use of OCT imaging in ultrafast ablation with a particularly convenient implementation<sup>[12]</sup>. The same light source is used to both cut and image, thus guaranteeing coaxial alignment. In addition to imaging where cut-

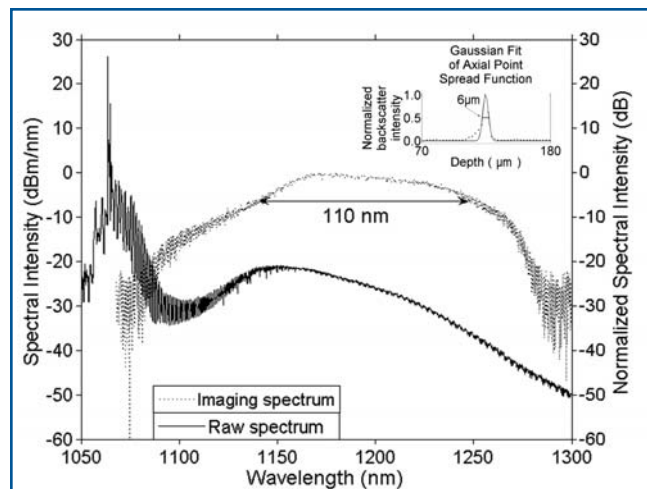


Fig. 3 Spectrum before (black curve, left axis) and after (dotted curve, right axis) filtering. Inset: point-spread function with Gaussian fit showing axial resolution.

ting is occurring, we also are sure of imaging when cutting is ongoing. As such we are sensitive to short-lived transients that would not be observable using nonsynchronized or CW imaging. The laser system used is a compact, modelocked fibre oscillator coupled to a single-pass ytterbium double-clad fibre amplifier. The spectrum (Fig. 3) has a wide shoulder, likely due to stimulated Raman scattering in the amplifier stage. We specifically exploit the broad bandwidth shoulder to provide high axial resolution OCT imaging. The strong peak at 1064 nm is removed by spectral filtering in the spectrometer to leave a relatively smooth profile with a bandwidth of 110 nm (Fig. 3, - normalized scale), allowing us to achieve a 6  $\mu\text{m}$  axial resolution (inset of Fig. 3).

Figure 4 shows a typical micromachining run on 304 stainless steel with 20 ps, 1.0  $\mu\text{J}$  pulses incident on the sample (spot size 14  $\mu\text{m}$ ) at a repetition rate of  $\sim 9$  MHz. The y-axis corresponds to depth into the sample (with the machining/imaging light incident from the top), and the x axis corresponds to time from the start of the run (temporal resolution set by the 46 kHz line rate of the infrared spectrometer). This type of depth vs. time functional OCT scan is known as OCT M-mode. Detector saturation does occur at early times obscuring some axial scans. The major feature apparent in the M-mode image is the

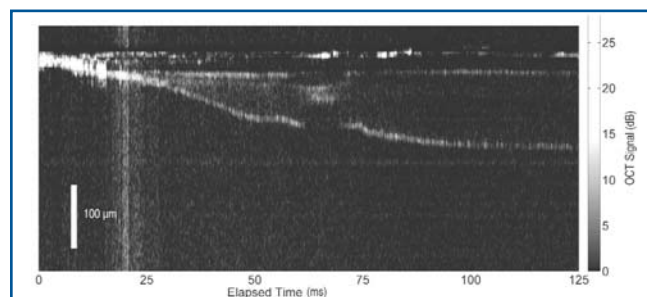


Fig. 4 304 stainless steel undergoing laser micromachining.

machining front descending into the sample as material is removed. The light's penetration depth into metal is much less than the axial resolution, so all the backscatter is coming from the bottom of the hole, the sidewalls or the surface. As such, the single axial scan does provide information about hole morphology, including intermediate sidewall features formed as machining progresses.

Though similar cut profiles are obtained for identical experimental parameters, the exact dynamics varies from run to run. Cut speed is extremely variable during the run. In addition, the bottom of the hole sometimes disappears (~62 ms in Fig. 4) at the same time as a diffuse layer appears at shallower depths inside the hole. The hole bottom reappears when the diffuse layer disappears, and cutting resumes. This intermittent effect could be due to the formation of a plasma of sufficient density to block the cutting/imaging laser. The stochastic nature of the

process is likely related to the high repetition rate of the machining laser (~9 MHz) and inhomogeneities of the steel.

## CONCLUSION

Ultrafast optical technology in combination with optical coherence tomography provide improved 3D imaging, as well as new possibilities and better understanding of laser micromachining.

## ACKNOWLEDGEMENTS

Funding for this work was provided by the Natural Sciences and Engineering Research Council, the Canadian Foundation for Innovation, the Ontario Ministry for Research and Innovation, the Ontario Centres of Excellence, and the Cancer Imaging Network of Ontario, supported by Cancer Care Ontario.

## REFERENCES

1. A.F. Fercher, W. Drexler, C.K. Hitzenberger and T. Lasser, "Optical coherence tomography-principles and applications", *Rep. Prog. Phys.*, **66**, 239-303 (2003).
2. R.B. Rosen, M. Hathaway, J. Rogers, J. Pedro, P. Garcia, P. Laissue, G.M. Dobre, and A.G. Podoleanu, "Multidimensional en-Face OCT imaging of the retina", *Opt. Express*, **17**, 4112-4133 (2009).
3. R. Huber, D.C. Adler, and J.G. Fujimoto, "Buffered Fourier domain mode locking: Unidirectional swept laser sources for optical coherence tomography imaging at 370,000 lines/s", *Opt. Lett.*, **31**, 2975-2977 (2006).
4. B. Potsaid, I. Gorczynska, V.J. Srinivasan, Y. Chen, J. Jiang, A. Cable, and J.G. Fujimoto, "Ultra-high speed spectral / Fourier domain OCT ophthalmic imaging at 70,000 to 312,500 axial scans per second", *Opt. Express*, **16**, 15149-15169 (2008).
5. B. Povazay, B. Hofer, C. Torti, B. Hermann, A.R. Tumlinson, M. Esmaelpour, C.A. Egan, A.C. Bird, and W. Drexler, "Impact of enhanced resolution, speed and penetration on three-dimensional retinal optical coherence tomography", *Opt. Express* **17**, 4134-4150 (2009).
6. W. Drexler, U. Morgner, R.K. Ghanta, F.X. Kärtner, J.S. Schuman, and J.G. Fujimoto, "Ultra-high-resolution ophthalmic optical coherence tomography", *Nature Medicine*, **7**, 502-507 (2001).
7. D.L. Marks, A.L. Oldenburg, J.J. Reynolds, and S.A. Boppart, "Autofocus algorithm for dispersion correction in optical coherence tomography", *App. Opt.*, **42**, 3038-3046 (2003).
8. B. Povazay, K. Bizheva, B. Hermann, A. Unterhuber, H. Sattmann, A.F. Fercher, W. Drexler, C. Schubert, P.K. Ahnelt, M. Mei, R. Holzwarth, W.J. Wadsworth, J.C. Knight, and P.S.J. Russel, "Enhanced visualization of choroidal vessels using ultrahigh resolution ophthalmic OCT at 1050 nm", *Opt. Express*, **11**, 1980-1986 (2003).
9. M.S. Muller, P.J.L. Webster and J.M. Fraser "Time-gated Fourier-domain optical coherence tomography," *Opt. Lett.*, **32**, 3336-3338 (2007).
10. M.S. Muller and J.M. Fraser, "Contrast improvement in Fourier-domain optical coherence tomography through time gating", *JOSA:A* (in press).
11. B.N. Chichkov, C. Momma, S. Nolte, F. von Alvensleben, and A. Tunnermann "Femtosecond, picosecond and nanosecond laser ablation of solids", *Appl. Phys. A*, **63** 109-115 (1996).
12. P.J.L. Webster, M.S. Muller, and J.M. Fraser "High speed in situ depth profiling of ultrafast micromachining", *Opt. Express*, **15**, 14967-14972 (2007).